



Pyruvate transporter BnaBASS2 impacts seed oil accumulation in *Brassica napus*

Shan Tang^{1,2}, Ning Guo^{1,2}, Qingqing Tang^{1,2}, Fei Peng^{1,2}, Yunhao Liu^{1,2}, Hui Xia^{1,2}, Shaoping Lu^{1,2}  and Liang Guo^{1,2,3,4,*} 

¹National Key Laboratory of Crop Genetic Improvement, Huazhong Agricultural University, Wuhan, China

²Hubei Hongshan Laboratory, Wuhan, China

³Shenzhen Institute of Nutrition and Health, Huazhong Agricultural University, Wuhan, China

⁴Shenzhen Branch, Guangdong Laboratory for Lingnan Modern Agriculture, Genome Analysis Laboratory of the Ministry of Agriculture, Agricultural Genomics Institute at Shenzhen, Chinese Academy of Agricultural Sciences, Shenzhen, China

Received 17 May 2022;

revised 22 August 2022;

accepted 29 August 2022.

*Correspondence (Tel 86-27-87286881; fax 86-27-87286885; email guoliang@mail.hzau.edu.cn)

Summary

Bile acid: sodium symporter family protein 2 (BASS2) is a sodium-dependent pyruvate transporter, which transports pyruvate from cytosol into plastid in plants. In this study, we investigated the function of chloroplast envelope membrane-localized BnaBASS2 in seed metabolism and seed oil accumulation of *Brassica napus* (*B. napus*). Four BASS2 genes were identified in the genome of *B. napus*. *BnaA05.BASS2* was overexpressed while *BnaA05.BASS2* and *BnaC04.BASS2-1* were mutated by CRISPR in *B. napus*. Metabolite analysis revealed that the manipulation of *BnaBASS2* caused significant changes in glycolysis-, fatty acid synthesis-, and energy-related metabolites in the chloroplasts of 31 day-after-flowering (DAF) seeds. The analysis of fatty acids and lipids in developing seeds showed that *BnaBASS2* could affect lipid metabolism and oil accumulation in developing seeds. Moreover, the overexpression (OE) of *BnaA05.BASS2* could promote the expression level of multiple genes involved in the synthesis of oil and the formation of oil body during seed development. Disruption of *BnaA05.BASS2* and *BnaC04.BASS2-1* resulted in decreasing the seed oil content (SOC) by 2.8%–5.0%, while OE of *BnaA05.BASS2* significantly promoted the SOC by 1.4%–3.4%. Together, our results suggest that *BnaBASS2* is a potential target gene for breeding *B. napus* with high SOC.

Keywords: *Brassica napus*, pyruvate transporter, BASS2, seed oil content, lipids, metabolites.

Introduction

Pyruvate is a central intermediate of carbohydrate metabolism in plants. During seed germination of oil plants, pyruvate is an important intermediate metabolite involved in the conversion of lipids to sugars through gluconeogenesis and β -oxidation (Sattler et al., 2004). Moreover, pyruvate is the output of glycolysis of glucose. On one hand, pyruvate produced from glycolysis is transported across the mitochondrial membrane by the mitochondrial pyruvate carrier (MPC; Bricker et al., 2012; Herzig et al., 2012). Under the catalysis of mitochondrial pyruvate dehydrogenase, pyruvate is converted into acetyl-CoA, which further participates in the tricarboxylic acid cycle, connecting the metabolism of sugars, proteins, and lipids (Le et al., 2021; Tovar-Mendez et al., 2003). On the other hand, pyruvate produced from glycolysis is involved in cellular metabolic flux in the plastid. Under the catalysis of plastidial pyruvate dehydrogenase, pyruvate is converted into acetyl-CoA, which acts as a metabolic precursor for many plastid-localized biosynthetic pathways, such as methyl erythritol phosphate (MEP) pathway, branched-chain amino acids and fatty acid (FA) pathway (Furumoto et al., 2011; Prabhakar et al., 2010; Weber and Linka, 2011). Thus, pyruvate is a vital intermediate connecting sugar, lipid, and amino acid metabolism of plants.

In plants, there are two pathways for supplying pyruvate to the plastid. The first way is to catalyse phosphoenolpyruvate (PEP) to produce pyruvate by plastidial pyruvate kinase (PKp) in the plastid

(Andre et al., 2007; Baud et al., 2007b; Prabhakar et al., 2010). Another way is to convert PEP into pyruvate by cytosolic pyruvate kinase (PKc) in the cytosol. Cytosolic pyruvate is then transported into the plastid via the pyruvate transporter (Eastmond and Rawsthorne, 2000; Prabhakar et al., 2010; Weber and Linka, 2011). Plastidial pyruvate plays an important role in FA and other metabolic pathways during seed development. In Arabidopsis, PKp consists of three subunits α , $\beta 1$, and $\beta 2$. Disruption of PKp resulted in defects in seed oil accumulation, FA synthesis, embryo elongation, and seed germination (Andre et al., 2007; Andre and Benning, 2007; Baud et al., 2007b). In rice, OsPKp consists of four subunits $\alpha 1$, $\alpha 2$, $\beta 1$ and $\beta 2$, mutation of *OsPKp1* would affect endosperm starch/FA biosynthesis, granule formation, grain filling, and seed germination (Cai et al., 2018a,b). In *Brassica napus* (*B. napus*), plastids were isolated from embryos of 23, 32, and 41 day-after-anthesis (DAA). Metabolic fluxes for oil synthesis were measured and the activity of the plastidial pyruvate transporter was increased by 19-fold and the utilization of plastidial pyruvate for FA synthesis was increased by 25-fold at 41 DAA (Eastmond and Rawsthorne, 2000). Thus, the above advances reveal that plastidial pyruvate plays an important role in seed development, especially in oil accumulation.

Bile acid: sodium symporter family protein 2 (BASS2) is a chloroplast envelope membrane-localized sodium-dependent pyruvate transporter that transports pyruvate from cytosol to plastid. This process is involved in the photosynthesis of C4 plants

and the MEP pathway of C3 plants (Furumoto, 2016; Furumoto et al., 2011). In Arabidopsis, disruption of *BASS2* resulted in mevastatin-sensitive phenotype, and the phenotype could be recovered by constitutive expression of *BASS2* in wheat and Arabidopsis, indicating that *BASS2* functions in supplying pyruvate to the MEP pathway (Furumoto et al., 2011; Zhao et al., 2016). In addition to the role in the MEP pathway, supplying pyruvate to plastid from cytosol via *BASS2* is reported to impact FA biosynthesis and seed oil accumulation. Seed-specific overexpression (OE) of *BASS2* resulted in 10%–37% more oil in Arabidopsis seeds (Lee et al., 2017). Nevertheless, beyond the confirmation that *BASS2* affects the phenotype of Arabidopsis seed oil accumulation, *BASS2*'s impact on pyruvate content in plastid and seed metabolism has not been revealed.

In this study, four plastidial *BASS2* proteins were identified in *B. napus*. The gene function and molecular mechanism of *BnaBASS2* on seed oil accumulation were investigated using OE and CRISPR mutants of *BnaBASS2*. These results suggest that *BnaBASS2* has a significant impact on seed metabolism and seed oil accumulation in *B. napus*.

Results

Generation of *BnaBASS2* OE and CRISPR mutant lines

To investigate the function of *BASS2*s in *B. napus*, the amino acid sequences of Arabidopsis *BASS2* were used for BLAST analysis in BnTIR database (<http://yanglab.hzau.edu.cn/BnTIR>; Liu et al., 2021). The results show that there are four homologous copies of *BASS2* (BnaA05G0069700ZS, designated as *BnaA05.-BASS2*; BnaC04G0079100ZS, designated as *BnaC04.BASS2-1*; BnaA04G0248500ZS, designated as *BnaA04.BASS2*; and BnaC04G0563700ZS, designated as *BnaC04.BASS2-2*), and they all exhibited more than 85% homology with AtBASS2. Among the four genes, *BnaA05.BASS2* is the most homologous to *BnaC04.BASS2-1* with a homology of 98%. *BnaA04.BASS2* is the most homologous to *BnaC04.BASS2-2* with a homology of 97% (Figures 1a and S1). Next, the expression level of *BnaBASS2* in different tissues was collected from the BnTIR database (Liu et al., 2021). The results show that the expression level of *BnaA04.BASS2* and *BnaC04.BASS2-2* is very low in different tissues, while *BnaA05.BASS2* and *BnaC04.BASS2-1* have higher expression in multiple tissues, especially in developing siliques and seeds (Figure 1a).

BASS2 was predicated to be a membrane protein with nine transmembrane regions (Figure S1). In this research, BnaA05.-*BASS2* fused with GFP at its C-terminus was transiently expressed in the epidermal cells of tobacco and protoplasts of Arabidopsis. The green fluorescence signal is found to encapsulate the autofluorescence of chloroplast membrane, suggesting that BnaA05.-*BASS2* is localized on the chloroplast membrane (Figures 1b and S2). The result was consistent with previous studies (Furumoto et al., 2011).

BnaA05.BASS2, having a much higher expression level than the other three homologous genes in developing silique and seed, was overexpressed in *B. napus* driven by 35S promoter. Four transgenic lines with increased expression of *BnaA05.-BASS2* in the seeds at 24 day-after-flowering (DAF) are successfully obtained (Figure 1c). Western blot using Flag antibody confirms that positive OE plants are acquired (Figure 1d). OE2 and OE5 having high expression at transcription and protein levels were used for further analysis in this study.

CRISPR/Cas9 was utilized to create mutants of *BnaBASS2*s. As a result, two homozygous mutants CR253 and CR313 with mutations in *BnaA05.BASS2* and *BnaC04.BASS2-1* are identified by sequencing and the mutations in *BnaA05.BASS2* and *BnaC04.BASS2-1* caused premature termination (Figures 1e and S3).

BnaBASS2 has significant effects on seed metabolism

It has been hypothesized and partially verified that pyruvate produced by glycolysis could be transported into the chloroplast via *BASS2* (Furumoto et al., 2011; Schwender et al., 2004; Weber and Linka, 2011). A brief model of carbon influx from the glycolysis pathway into FA synthesis is shown in Figure 2a. To explore the impact of pyruvate transporter *BASS2* on seed metabolism of *B. napus*, metabolites were extracted from 31 DAF seeds and determined by liquid chromatography with tandem mass spectrometry (LC–MS/MS) method. The results show that significant changes occur in most glycolytic and FA synthesis metabolites in the seeds of OE and mutant lines (Figure 2b). In the whole seeds, the contents of the metabolites of glucose-6-phosphate (G6P), fructose-6-phosphate (F6P), fructose-1,6-diphosphate (FBP), dihydroxy-acetone-phosphate (DHAP), 3-phosphoglycerate (3-PGA), PEP and pyruvate (Pyr) related to glycolysis are significantly lower in CR253 than that in WT. However, most of them are higher in OE5 than that in WT, except that the content of G6P, F6P, and 3-PGA have no difference between OE5 and WT. Acetyl-CoA and malonyl-CoA are the precursors for FA synthesis. Compared with WT, the contents of acetyl-CoA and malonyl-CoA are lower in CR253 than that in WT. Nevertheless, the content of acetyl-CoA is higher, but there has been no change in malonyl-CoA in OE5 (Figure 2b). Additionally, intact chloroplasts were separated from 31 DAF seeds by the sucrose gradient method (Figure S4). In chloroplast, the contents of the metabolites of G6P, F6P, FBP, DHAP, 3-PGA, PEP, and Pyr related to glycolysis, and acetyl-CoA and malonyl-CoA related to FA synthesis are significantly lower in CR253 than that in WT. Whereas, the level of those metabolites are higher in OE5 except G6P and PEP (Figure 2c).

The synthesis of seed oil is an energetically costly process, which requires ATP, NADH, and NADPH for carbon flux. Glycolysis is a significant source of ATP, NADH, and NADPH. In chloroplast, light energy can be utilized for ATP and NADPH synthesis, which is required by FA synthesis (Judge and Dodd, 2020; Pfeil et al., 2014; Rawsthorne, 2002). The levels of ATP, ADP, NAD(P), and NAD(P)H in whole seeds and isolated chloroplasts of 31 DAF seeds were determined by LC–MS/MS method. In whole seeds, the contents of ATP, NADH, and NADPH are significantly increased in OE5 but decreased in CR253 compared with WT. However, the content of ADP, NAD and NADP are significantly decreased in OE5 but elevated in CR253 except no significant change of NADP in CR253 compared with WT (Figure 3a–c). In chloroplast, compared with WT, the contents of ATP, NADH, and NADPH are significantly increased in OE5 but decreased in CR253 except no significant change of ATP and NADH in CR253. The contents of ADP, NAD, and NADP are significantly decreased in OE5 but elevated in CR253. However, there is no significant change in NADP in OE5 and CR253 (Figure 3d–f).

The ratios of energy metabolites were used to evaluate the energy charge and reducing power in WT, OE, and mutant lines. In whole seeds, ATP/ADP, NADH/NAD, and NADPH/NADP are

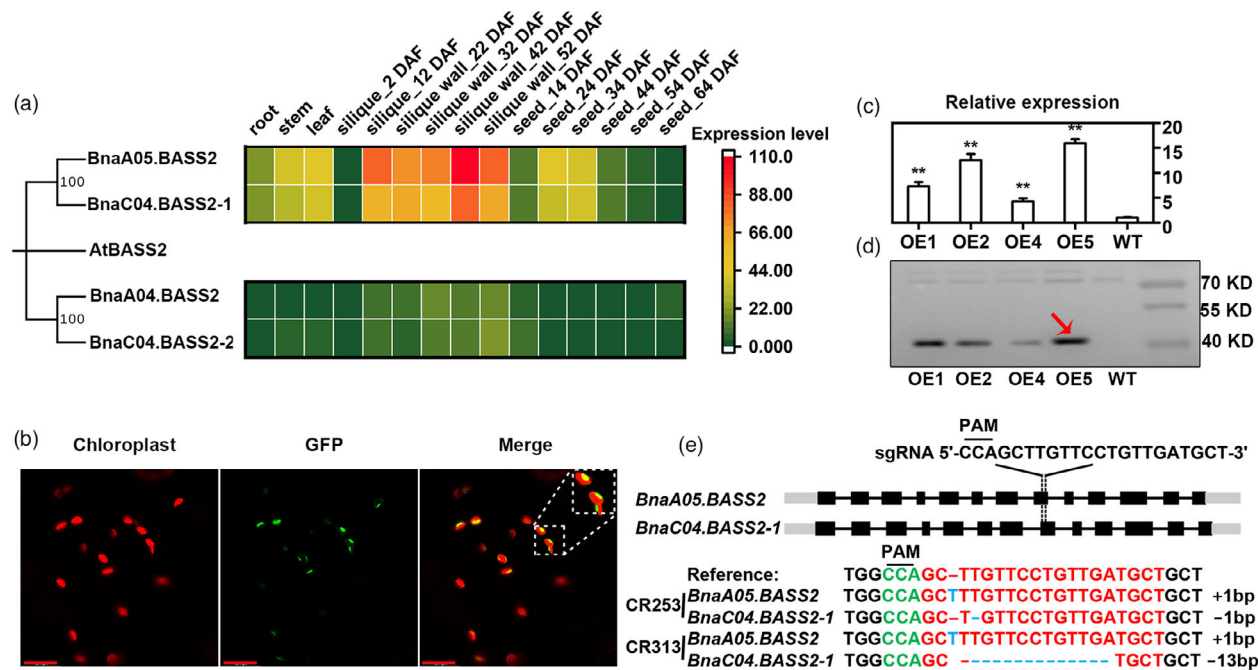


Figure 1 Generation of overexpression (OE) plants and knockout mutants of *BnaBASS2*. (a) Gene expression of *BASS2*s in *Brassica napus* tissues. At, *Arabidopsis thaliana*; Bn, *B. napus*; Gene expression data are from BnTIR (<http://yanglab.hzau.edu.cn/>). (b) *BnaA05.BASS2* is a chloroplast membrane protein by the observation of tobacco epidermal cells under confocal. Bars = 17 μ m. (c) Relative expression level of *BnaA05.BASS2* in OE lines by quantitative real-time PCR. Total RNA was extracted from 24 DAF seeds. Values are means \pm SD ($n = 3$). ** indicates $P < 0.01$, based on a student t -test. (d) Expression of the *BnaA05.BASS2* in OE lines by Western blot using Flag antibody. The size of the target protein with Flag tag is 45 KD and the red arrow indicates the target protein band. Protein was extracted from 24 DAF seeds. (e) Acquisition of mutant lines based on CRISPR/Cas9 technology. CRISPR targets the eighth exon of *BnaA05.BASS2* and *BnaC04.BASS2-1*. CR253 and CR313 are homozygous double mutants of *BnaA05.BASS2* and *BnaC04.BASS2-1*.

much higher in OE5 but lower in CR253, except for NADPH/NADP in CR253, which is comparable with WT. In chloroplast, ATP/ADP, NADH/NAD, and NADPH/NADP are also much higher in OE5 but lower in CR253, except for NADH/NAD in CR253, which is comparable with WT. Interestingly, the ATP/ADP, NADH/NAD, and NADPH/NADP in the whole seeds of OE5 are changed from 3.8, 2.6, and 2.1 to 16.9, 0.03, and 4.3 in the chloroplast of OE5. ATP/ADP, NADH/NAD, and NADPH/NADP in the whole seeds of CR253 are changed from 0.8, 0.4, and 1.1 to 0.6, 0.008, and 0.5 in the chloroplast of CR253, respectively (Figure 3a–f). The above results indicate that *BnaBASS2* affects multiple metabolic pathways including glycolysis, FA synthesis, and energy metabolism in the seeds.

***BnaBASS2* promotes oil accumulation during seed development**

Developing seeds were collected and FAs at 21, 27, 31, 36, 41, and 55 DAF were extracted and quantified by the gas chromatography-flame ionization detector (GC-FID) method. Compared with WT, OE5 has a higher level of oil, while the mutant CR253 exhibits a lower level in the process of seed oil accumulation (Figure 4a). The data of seed weight and oil per seed were obtained by calculating the total number of seeds and seed weight. The results revealed that compared with WT, OE5's seed weight has no significant difference, but the mutant CR253 shows a decreased weight, especially at the seed maturation stage (Figure 4b).

Lipidome analysis of 31 DAF seeds showed that triacylglycerol (TAG) is increased by 57.1% in OE5 but decreased by 51.1% in CR253 compared with WT. The content of DAG is increased by 18.0% in OE5 while has no obvious difference in CR253 compared with WT. Moreover, compared with WT, the content of other lipids MGDG, DGDG, PC, PE, and PA has no obvious difference between WT, OE5, and CR253 (Figure 4c). The content of TAG species -52:2, -54:2, -54:3, -54:6, -54:7, -56:2, -56:3, and -56:4 is increased in OE5, but the content of TAG-52:2, -52:3, -52:5, -54:2 to -54:7, -56:2, -56:3, and -56:4 is decreased in CR253 (Figure 4d). Compared with WT, the content of DAG species -34:0, -34:2, -34:4, -36:1, -36:3, -36:4, -36:5, and -36:6 is increased in OE5, but the content of DAG-36:3 is decreased in CR253 (Figure 5).

Furthermore, the expression of some key genes related to FA synthesis, TAG synthesis, and oil body (OB) formation was analysed in 31 DAF seeds of WT, OE5, and CR253. The results showed that the expression of *WRINKLED1* (*WRI1*), a master regulator in the glycolytic pathway, and FA biosynthesis (Adhikari *et al.*, 2016, Baud *et al.*, 2009, Kong and Ma, 2018, Kong *et al.*, 2019, To *et al.*, 2012, Yang *et al.*, 2022), is elevated by 25.8% in OE5 but reduced by 31.8% in CR253 compared with WT. Compared with WT, the expression of FA synthesis-related genes *malonyltransferase* (*MCMT*), *enoyl-ACP reductase* (*ENR*), and *acyl-ACP thioesterase A* (*FATA*) is decreased by 34.3%, 68.2%, and 28.9% in CR253. In OE5, *MCMT* and *FATA* are increased by 22.9% and 30.8%, but *ENR* shows no change. The

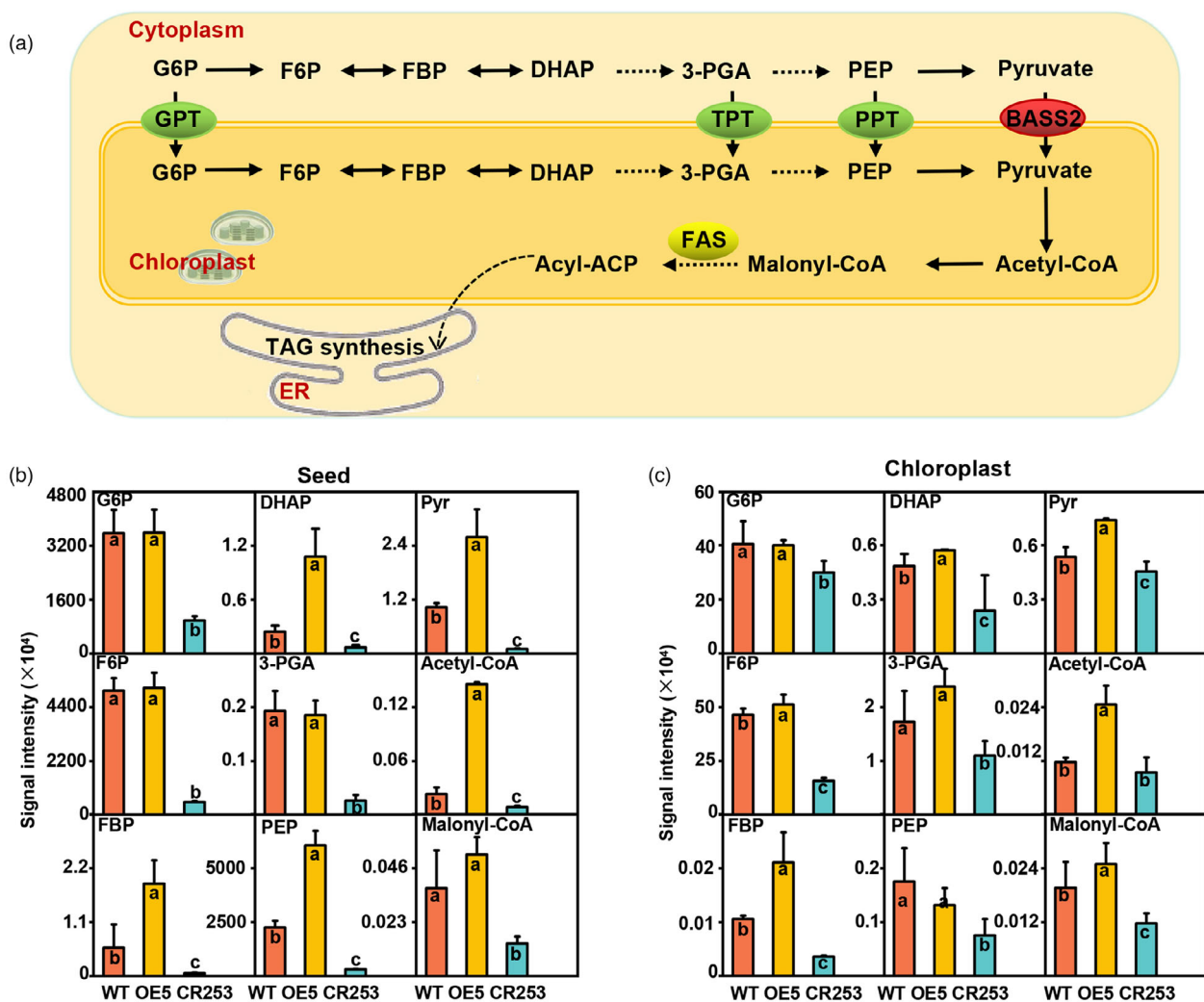


Figure 2 *BnaBASS2* impacts glycolysis and fatty acid (FA) pathways in developing seeds. (a) Brief diagrams of the glycolytic pathway and FA synthesis in the plant. (b) The total content of G6P, F6P, FBP, DHAP, 3-PGA, PEP, Pyr, Acetyl-CoA, and Malonyl-CoA in 31 DAF seeds. (c) The content of G6P, F6P, FBP, DHAP, 3-PGA, PEP, Pyr, Acetyl-CoA, and Malonyl-CoA in the separated chloroplasts of 31 DAF seeds. 3-PGA, 3-phosphoglycerate; BASS2, pyruvate transporter named bile acid:sodium symporter family protein 2; DHAP, dihydroxy-acetone-phosphate; F6P, fructose-6-phosphate; FBP, fructose-1,6-diphosphate; G6P, glucose-6-phosphate; GPT, glucose 6-phosphate translocator; PEP, phosphoenolpyruvate; PPT, phosphoenolpyruvate/phosphate translocator; Pyr, pyruvate; TPT, triose phosphate translocator; values are mean \pm SD ($n = 6-8$). Different letters represent significant differences at $P < 0.05$, based on an ANOVA analysis with the Fisher LSD test.

expression of genes related to TAG synthesis such as *glycerol-3-phosphate dehydrogenase (GPDH)*, *glycerol-3-phosphate acyltransferase 9 (GPAT9)*, *lysophosphatidic acid acyltransferase 1 (LPAAT1)*, *lysophosphatidic acid acyltransferase 2 (LPAAT2)*, *diacylglycerol acyltransferase 1 (DGAT1)*, *diacylglycerol acyltransferase 2 (DGAT2)*, *lysophosphatidylcholine acyltransferase (LPCAT)* and *CDP-choline:diacylglycerol cholinephosphotransferase (CPT)* is lower in CR253 than that in WT, while they have higher expression in OE5. Moreover, the expression level of genes related to OB formation such as *oil body oleosin 1 (OBO1)*, *oil body oleosin 2 (OBO2)*, *oil body oleosin 3 (OBO3)*, and *caleosin (CALO)* is also determined. The data show that all of them had lower expression in CR253. In detail, *OBO1*, *OBO2*, *OBO3*, and *CALO* are decreased by 82.0%, 94.9%, 76.1%, and 85.1% in CR253 than that in WT. *OBO1*, *OBO3*, and *CALO1* are increased by 22.9%, 91.6%, and 46.2% in OE5 than that in WT except that

there is no difference in *OBO2* (Figure 4e). The expression level of several genes in the glycolytic pathway, including *hexokinase 1 (HK1)*, *phosphofructokinase 1 (PFK1)*, *plastidic pyruvate kinase (pPK1 and pPK3)*, and *cytosolic pyruvate kinase (cPK1 and cPK2)*, which control rate-limiting steps of the glycolytic pathway, were determined (Figure S6). The results show that the expression levels of all of the above genes are significantly increased in *BnaBASS2* mutant CR253. However, except for *HXX*, the expression of other genes is down-regulated in the OE5. Thus, the above results suggest that *BnaBASS2* promotes oil accumulation and expression level of genes involved in seed oil synthesis during seed development.

BnaBASS2 impacts seed oil content in mature seeds

Seed oil content-related traits of mature seeds were also investigated. Three-year (Year 2019, 2020, and 2021) of near-

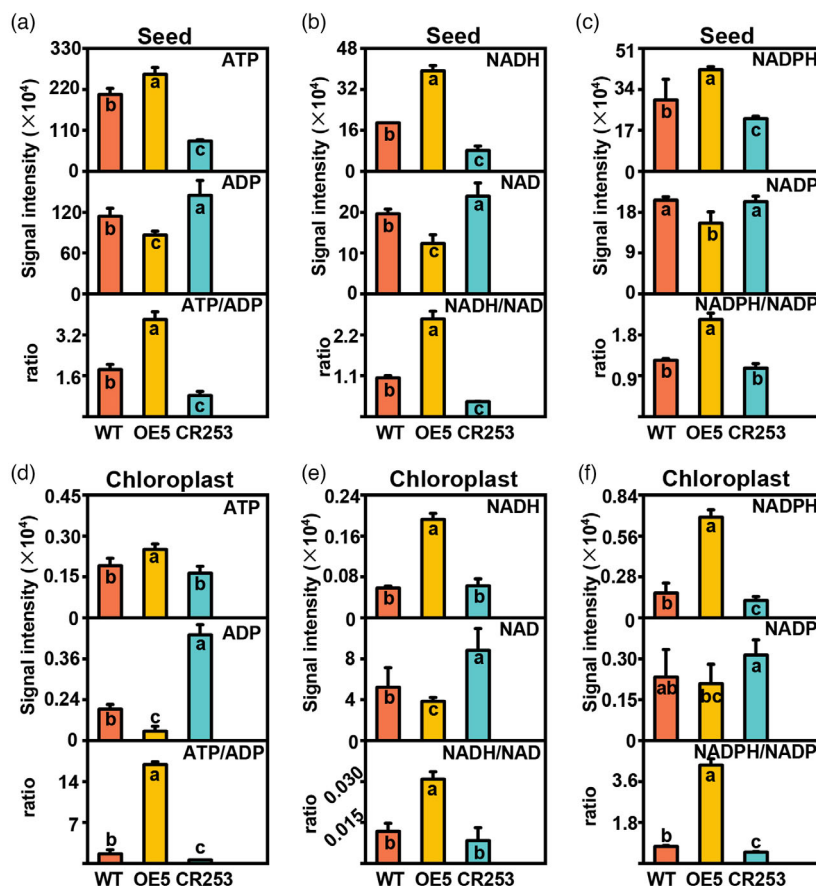


Figure 3 Metabolic impact of *BnaBASS2* on ATP/ADP, NADH/NAD, and NADPH/NADP in developing seeds. (a) ATP content, ADP content, and ATP/ADP in 31 DAF seeds. (b) NADH content, NAD content, and NADH/NAD in 31 DAF seeds. (c) NADPH content, NADP content, and NADPH/NADP in 31 DAF seeds. (d) ATP content, ADP content, and ATP/ADP in separated chloroplasts of 31 DAF seeds. (e) NADH content, NAD content, and NADH/NAD in separated chloroplasts of 31 DAF seeds. (f) NADPH content, NADP content, and NADPH/NADP in separated chloroplasts of 31 DAF seeds. Values are mean \pm SD ($n = 6-8$). Different letters represent significant differences at $P < 0.05$, based on an ANOVA analysis with the Fisher LSD test.

infrared spectrometer (NIRS) data display that SOC of OE is increased by 1.4%–3.4%, while SOC of two CRISPR mutants is reduced by 2.8%–5.0% compared with WT (Figure 5a). To confirm the results of NIRS, FAs in mature seeds were analysed by GC-FID. Compared with WT, SOC of OE2 and OE5 is elevated by 2.1% and 4.7%, while CR253 and CR313 are reduced by 4.3% and 6.7% (Figure 5b). In addition, the FA composition shows that the content of palmitic acid (C16:0), stearic acid (C18:0), and linoleic acid (C18:2) is slightly reduced, and oleic acid (C18:1) is slightly increased in OE, while C18:2 is slightly increased and C20:1 is reduced in the mutants (Figure S7).

TAG is the predominant lipid in mature seeds. The content of TAG is increased by 12.2% in OE5 and reduced by 11.4% in CR253, compared with WT (Figure 5c). Compared with WT, the content of TAG species -52:3, -52:4, -54:5 to -54:7, -56:2 to -56:5 is increased in OE5, but the content of TAG-52:2 to -52:3 and -54:2 to -54:5 is decreased in CR253 (Figure 5d).

Oil bodies are the place for TAG storage. Compared with WT, the density of OBs is obviously less in mutant CR253, while OE5 exhibits the opposite trend. The area of protein bodies is larger in CR253 but smaller in OE5 (Figure 5e). Moreover, the number of OBs and the size of OBs were quantified and compared among WT, OE5, and CR253. Compared with WT, OE5 had fewer OBs in 100 μm^2 while

CR253 has more OBs. The total area of OBs is 100 μm^2 and the size per OB are larger in OE5 but smaller in CR253 (Figure 5f–h).

Moreover, other seed-related traits such as protein, soluble sugar, and starch content were measured. Compared with WT, the protein content in OE2 and OE5 is noticeably decreased by 1.7% and 1.8%, while it is increased by 2.7% and 2.2% in CR253 and CR313 (Figure S8a). The soluble sugar is decreased in OE lines but increased in mutants (Figure S8b). The starch content is decreased in mutants, but there is no change in OE lines (Figure S8c). Taken together, the above results suggest that *BnaBASS2* is important for seed oil accumulation in *B. napus*.

The effects of *BnaBASS2* on plant growth

The seeds of WT, OE, and mutant lines were sown in the pots in the growth chamber and their growth phenotypes at 20, 40, and 80 days were observed. It shows that both OE and mutant lines are grown normally, and no significant growth phenotypic differences are observed (Figure S9a–c). To further evaluate the growth, several growth-related traits were measured for 40-day-old plants. The content of chlorophyll a (Chla), chlorophyll b (Chlb), and carotenoid (Car) is comparable between WT, OE, and mutant lines (Figure S10a). Compared with WT, the leaves of OE lines have a higher level of soluble sugars, whereas the mutants

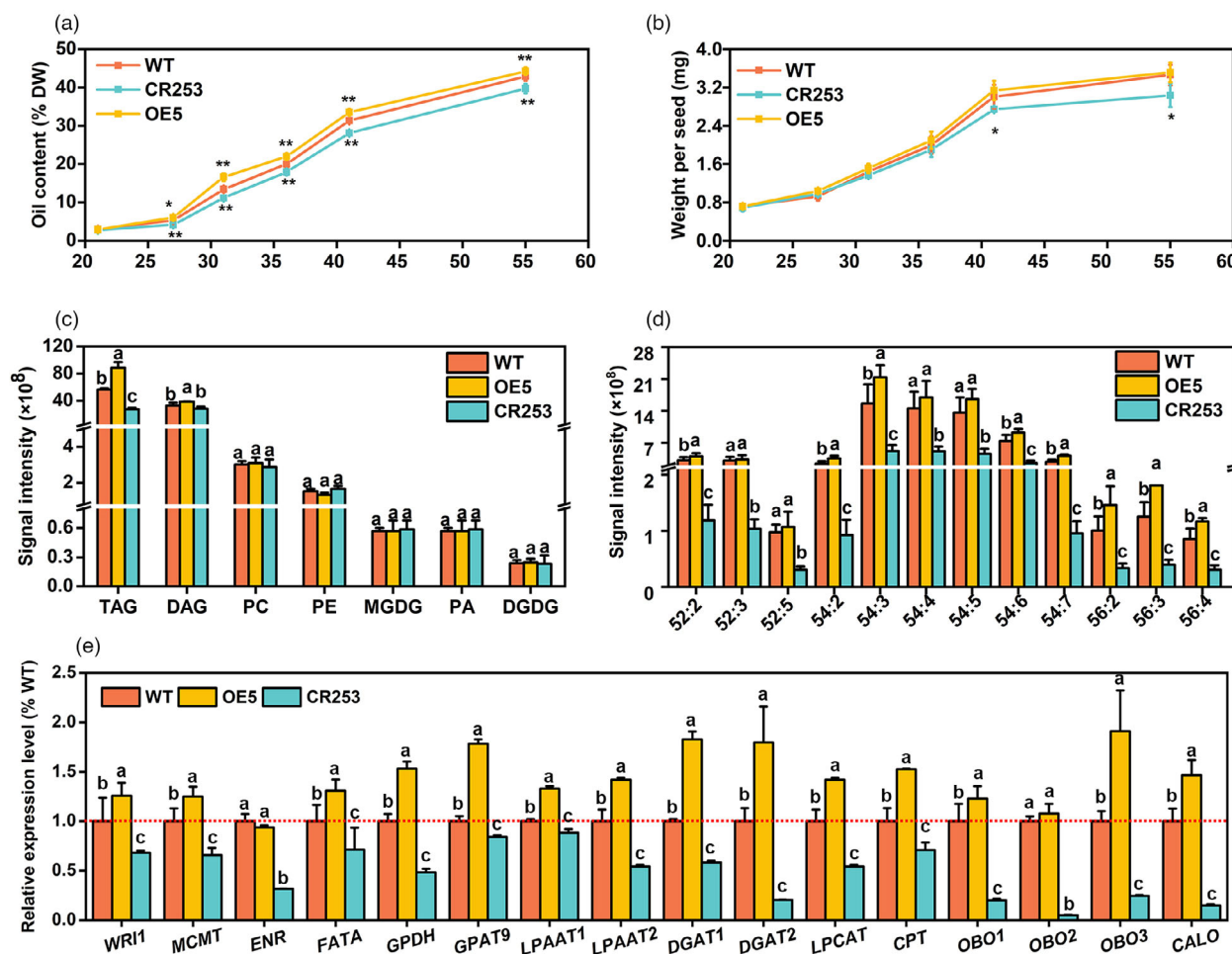


Figure 4 *BnaBASS2* contributes to oil accumulation during seed development. (a, b) Oil content and weight per seed of developing seeds. Oil content and oil per seed were measured by the GC-FID method. Seeds were obtained at 21, 27, 31, 36, 41, and 55 DAF. Values are mean \pm SD ($n = 4-6$). ** indicates $P < 0.01$, based on a student *t*-test. (c) and (d), Content of polar lipids and TAG species content in 31 DAF seeds. Values are means \pm SD ($n = 6-8$). Different letters represent significant differences at $P < 0.05$, based on an ANOVA analysis with the Fisher LSD test. (e) The expression level of genes involved in seed oil synthesis. *CALO*, caleosin; *CPT*, CDP choline:diacylglycerol cholinephosphotransferase; *DGAT1*, diacylglycerol acyltransferase 1; *DGAT2*, diacylglycerol acyltransferase 2; *ENR*, enoyl-ACP reductase; *FATA*, acyl-ACP thioesterase A; *GPAT9*, glycerol-3-phosphate acyltransferase 9; *GPDH*, glycerol-3-phosphate dehydrogenase; *LPAAT1*, lysophosphatidic acid acyltransferase 1; *LPAAT2*, lysophosphatidic acid acyltransferase 2; *LPCAT*, lysophosphatidylcholine acyltransferase; *MCMT*, malonyltransferase; *OBO1*, oil body oleosin 1; *OBO2*, oil body oleosin 2; *OBO3*, oil body oleosin 3; *WRI1*, wrinkled1. Total RNA was extracted from 31 DAF seeds. Relative expression level was calculated by comparison to actin's expression level. Values are means \pm SD ($n = 3$). Different letters represent significant differences at $P < 0.05$, based on an ANOVA analysis with the Fisher LSD test.

show the opposite trends (Figure S10b). Nevertheless, there is no difference in the starch content in the leaves among WT, OE, and mutant lines (Figure S10c). The biomass determination shows that there is no significant difference in fresh and dry weight among WT, OE, and mutant lines (Figure S10d). In addition, the photosynthetic efficiency was monitored. The results show that OE lines have a higher photosynthetic rate, transpiration rate, stomatal conductance, and intercellular CO₂ concentration than that in WT. However, mutant lines show the opposite (Figure S10e-h). These results suggest that *BnaBASS2* impacts sugar accumulation and plant photosynthesis in the leaves.

The impact of *BnaBASS2* on agronomic traits of *B. napus* was also evaluated. Plants were sown in the field and harvested at the mature stage. The agronomic traits including plant height, thousand seed weight and plant yield, etc. were investigated (Figure S11, Table S1). The results show that the value of most of

the agronomic traits has no significant change between OE lines and WT, except a slight decrease in the number of effective branches in OE2. Most of the agronomic traits are significantly lower in mutants than that in WT, except no obvious difference in plant height and number of effective branches. In detail, the silique number per plant, seed number per silique, thousand seed weight, and yield per plant of the mutants are reduced by 32.7%, 17.0%, 7.8%, and 26.8%, respectively. These results suggest that *BnaBASS2* is necessary for plant growth, and disruption of *BnaBASS2* can reduce rapeseed yields.

Discussion

The function of BASS2 is transporting pyruvate from cytosol to the plastid (Furumoto *et al.*, 2011). It's reported that the plastidial pyruvate is used for the MEP pathway and FA

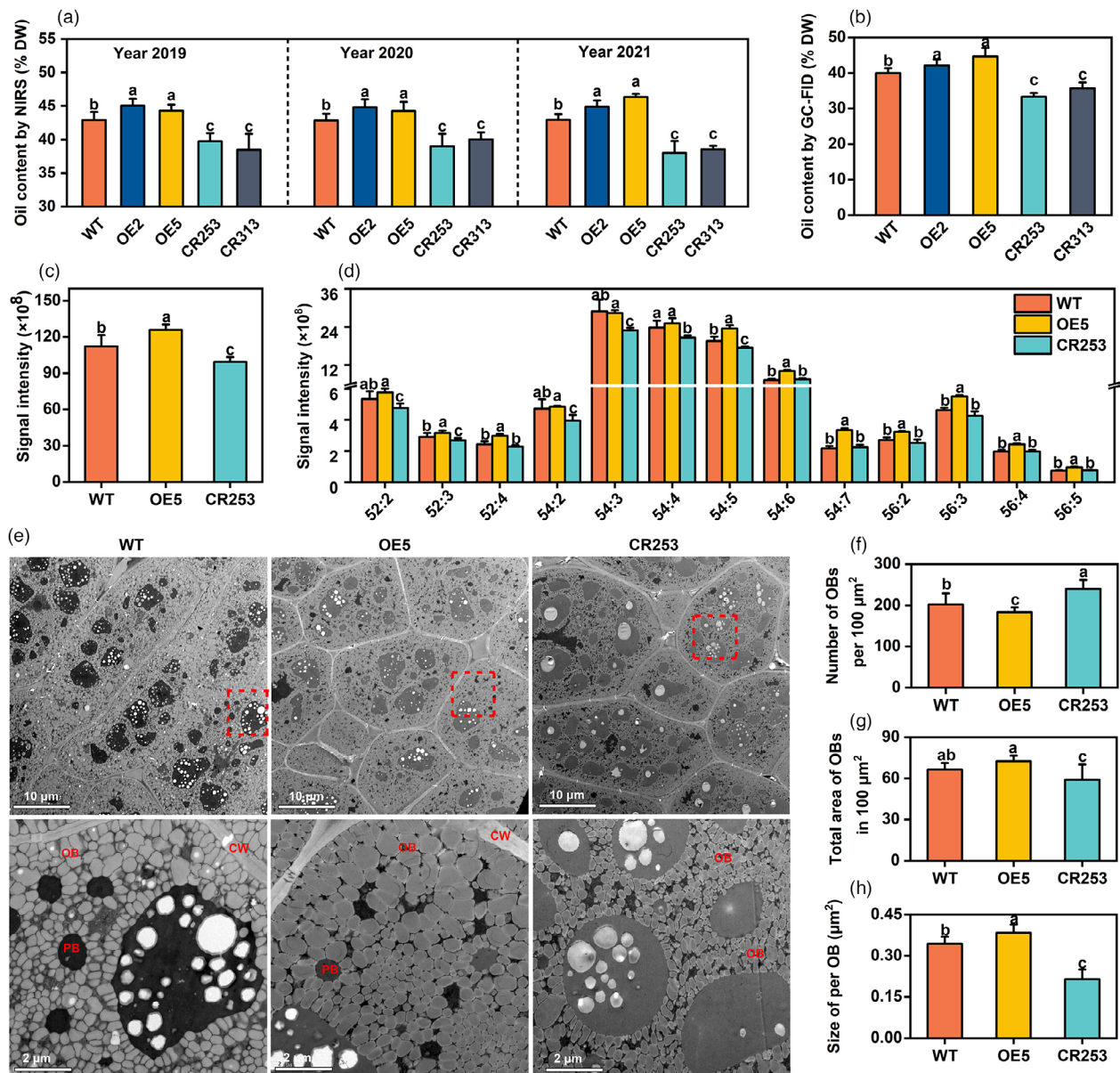


Figure 5 *BnaBASS2* promotes seed oil accumulation in mature seeds. (a) Oil content in mature seeds. Data were measured by NIR. Values are means \pm SD ($n = 4-6$). (b) Oil content in mature seeds. Data were determined by GC-FID. Values are means \pm SD ($n = 4-6$). (c) Contents of neutral lipids TAG. Values are means \pm SD ($n = 6-8$). (d) Triacylglycerol species content. Values are mean \pm SD ($n = 6-8$). (e) OBs of mature seeds were examined by scanning transmission electron microscopy. Bottom is a zoom-in on the red box of upper. (f-h) Number of OBs per 100 μm^2 , total area of OBs in 100 μm^2 , and size per OB in (e). Image J software was used to calculate the number and size of OBs. Values are mean \pm SD ($n = 12-16$). CW, cell wall; OB, oil body; PB, protein body. Different letters represent significant differences at $P < 0.05$, based on an ANOVA analysis with the Fisher LSD test.

biosynthesis (Furumoto *et al.*, 2011; Prabhakar *et al.*, 2010; Weber and Linka, 2011). Knockout of *BASS2* caused mevastatin-sensitive phenotype (Furumoto *et al.*, 2011; Zhao *et al.*, 2016), but it is not clear whether FA biosynthesis or oil accumulation is affected in *BASS2* mutant. In this study, it is the first time to report that the knockout of *BASS2* could reduce the SOC by 2.8%–5.0% in *B. napus*. Metabolites of seed plastid were determined and glycolysis- and FA-related metabolites were significantly decreased in the mutants of *BnaBASS2*. Meanwhile, a lower level of energy-related metabolites ATP and NAD(P)H was detected in the mutant (Figures 2 and 3). Previous studies found that *BASS2* showed sodium-dependent pyruvate uptake activity,

and the sodium influx was balanced by sodium:proton antiporter (NHD1), which was required for exporting sodium from the chloroplast to maintain the sodium gradient required for the import of pyruvate (Furumoto *et al.*, 2011). We hypothesize that disruption of *BnaBASS2* can block the supply of pyruvate to the plastid, which affects the process of photosynthesis, glycolysis pathway, etc. These processes are closely related to energy. Due to the decreased level of pyruvate and energy, FA synthesis in the plastid was reduced and the formation of TAG is suppressed. Multiple studies showed that *WRI1* is a master regulator in the glycolytic pathway, FA biosynthesis, and lipid metabolism (Adhikari *et al.*, 2016; Baud *et al.*, 2009; Kong *et al.*, 2019;

Kong and Ma, 2018; To *et al.*, 2012; Yang *et al.*, 2022). In our research, genes involved in the FA and oil biosynthesis of seed were significantly increased in OE lines and decreased in mutants (Figure 4f). Increased SOC of OE lines and decreased SOC of mutant lines might result from the regulation of *WRI1*, which affects the glycolysis, FA synthesis, TAG synthesis, and OB formation in the process of seed oil accumulation. Hence, *BnaBASS2* could impact multiple pathways to regulate seed oil accumulation.

The metabolite level of the whole seeds was also significantly reduced in mutants, which may be caused by photosynthesis. Reduced photosynthesis in the mutants leads to a reduction in carbon sources and thus a decrease in metabolite level. In this study, reduced photosynthesis was detected only in the leaves of mutants (Figure S10e–h), whether the photosynthesis of seeds is affected in mutants needs to be determined in the future. Source, sink, and flow are three important factors that determine crop yield, and high yield can only be achieved when the development of crops reaches sufficient source, large sink, and smooth flow (Adachi *et al.*, 2020; Wang *et al.*, 2021). In our research, photosynthesis was significantly reduced in the mutants, that is, the reduction in the source. Moreover, the number of silique number per plant, seed number per silique, and thousand seed weight were significantly reduced in mutants, that is, the reduction in the sink. Therefore, the yield reduction in the mutants may be caused by insufficient source and small capacity of the sink, which work together to limit the effects of push (source) and pull (sink). It is worth noting that, ultimately, the contents of sugar and protein are lower in OE seeds, while higher in mutants. And the content of starch is lower in mutants (Figure S8a–c). It indicates that more carbon flows into seed oil synthesis in OE lines.

In plants, there are several translocators that transport glycolysis metabolites from cytosol to plastid. Glucose 6-phosphate translocator (GPT), triose phosphate translocator (TPT), xylulose 5-phosphate translocator (XPT), and phosphoenolpyruvate translocator (PPT) transport G6P, 3-PGA, xylulose 5-phosphate, and PEP, respectively, from cytosol to plastid (Weber and Linka, 2011). Previous studies revealed that several plastidic phosphate translocators had an effect on plant growth and chloroplast development. *GPT1* was essential for pollen maturation and normal embryo sac development, the mutation of *GPT1* was lethal (Andriotis *et al.*, 2010; Niewiadomski *et al.*, 2005; Rolletschek *et al.*, 2007). The combined loss of *TPT* and *XPT* showed severe growth retardation (Hilgers *et al.*, 2018a, 2018b). Knockout of *PPT1* caused slower growth, yellowing leaf, and abnormal development of chloroplast (Li *et al.*, 1995; Streatfield *et al.*, 1999). However, in our study and previous studies, *BASS2*-deficient plants did not exhibit a visible vegetative growth phenotype under normal growth conditions (Figure S9). We speculate the main reason is that PEP metabolized by PKp in the plastid is the main source of plastidial pyruvate. In *Arabidopsis*, disruption of *PKp* could cause 60% reduction in seed oil, retarded embryo elongation, and seed germination (Andre *et al.*, 2007; Andre and Benning, 2007; Baud *et al.*, 2007b). At different stages of seed development in *B. napus*, the activity of PKp is slightly higher than that of PKc (Eastmond and Rawsthorne, 2000). In our study, although knockout of *BnaBASS2* resulted in blocked pyruvate transport from cytosol to plastid, another source of plastidial pyruvate could compensate for the pyruvate import deficiency in the *BnaBASS2* mutant. PPT1 transports PEP into the plastid, and PKp catalyses the synthesis of plastidial pyruvate, which is used for normal chloroplast

membrane lipid synthesis, thus maintaining normal growth. Our results suggest that loss of *BnaA05.BASS2* and *BnaC04.BASS2-1* resulted in a moderate yield penalty and a decrease in SOC in *B. napus*. Together, these results indicate that conversion of PEP to pyruvate by PKp provides a major source of pyruvate for metabolisms in the plastid.

Brassica napus is an important oil crop in the world, and improving oil production is one of the important goals of rapeseed breeding (Hua and Wang, 2016; Zou *et al.*, 2022). Biotechnology has been broadly used to improve the oil content in oil seeds. At present, metabolic engineering strategies to improve seed oil accumulation can be divided into upregulation of FA biosynthesis (Push), increasing TAG assembly (Pull), and increasing TAG storage/preventing breakdown. For example, overexpression of transcription factors such as *WRI1*, *LEC1*, and *LEC2* could improve seed oil accumulation by regulating genes involved in FA biosynthesis and functioning to 'Push' FA de novo synthesis (Baud *et al.*, 2007a; Liu *et al.*, 2010; Manan *et al.*, 2017; Mu *et al.*, 2008; Santos Mendoza *et al.*, 2005; Shen *et al.*, 2010; Tan *et al.*, 2011). Overexpression of DGAT improved seed oil by 'Pull' much more acyl chains to DAG for TAG biosynthesis (Jako *et al.*, 2001; Liu *et al.*, 2015a; Vanhercke *et al.*, 2013; Zhang *et al.*, 2018). Gene silencing of *Sugar-Dependent 1 (SDP1)* could enhance seed oil by blocking the degradation of TAG (Kelly *et al.*, 2013; Kim *et al.*, 2014). In our study, overexpression of *BnaBASS2* could significantly enhance the SOC in *B. napus* and had no obvious negative effect on agronomic traits. Thus, *BnaBASS2* is a potential gene for breeding *B. napus* with high oil content.

Materials and methods

Analysis of BASS2 in *B. napus*

The genomic sequence, amino acid sequence, and different tissue expression data of *BnaBASS2* were downloaded from BnTIR (<http://yanglab.hzau.edu.cn/>; Liu *et al.*, 2021). Phylogeny and amino acid sequence alignment of *BnaBASS2* were performed by MEGA7 and CLUSTALW (<https://www.genome.jp/tools-bin/clustalw>).

Subcellular localization

The CDS of *BnaA05.BASS2* was amplified and ligated into the pMDC83 vector, which contains a 2 × 35S promoter and a C-terminal GFP tag. The recombinant *BnaA05.BASS2::GFP* vector was transformed into the mesophyll protoplasts of *Arabidopsis* (Yoo *et al.*, 2007) and epidermal cells of tobacco (Yang *et al.*, 2021). The fluorescence pictures were observed using a Leica confocal microscope at 12 h after transfection.

Vector construction and plant transformation

To construct the OE vector of *BnaBASS2*, the CDS of *BnaA05.BASS2* was cloned and ligated into p35S-FAST. To create the mutants of *BnaBASS2*, CRISPR/cas9-mediated gene editing technique was utilized (Xing *et al.*, 2014). Briefly, two sgRNAs, which could both target *BnaA05.BASS2* and *BnaC04.BASS2-1*, were designed on the website (<http://cbi.hzau.edu.cn/cgi-bin/CRISPR>; Lei *et al.*, 2014). The amplified product by PCR including two sgRNAs was linked to pKSE401 vector using Golden Gate Assembly (Gao *et al.*, 2013).

The OE and mutant vectors of *BnaBASS2* were transformed into *Agrobacterium tumefaciens* GV3101, respectively. Genetic transformation of rapeseed was carried out by agrobacterium-

mediated method as described previously (Dai et al., 2020). Westar was utilized as a transformation receptor. The obtained OE plants were detected by PCR using specific primers.

RNA extraction and quantitative real-time PCR

30–50 mg developing seed was collected and total RNA was extracted using Easstep®Super Total RNA Extraction Kit (Promega Corporation, Madison, WI) (catalogue number LS1040). The quality of isolated RNA was determined by NanoDrop (Thermo Scientific, Waltham, MA) and 1.5% agarose gel electrophoresis, respectively. Then, 1–3 µg total RNA was used to synthesize cDNA with cDNA Synthesis SuperMix (TransGen, Beijing, China; catalogue number AE311). The synthesized cDNA was diluted 10 times, and then quantitative real-time PCR (qPCR) was conducted with an ABI 7500 system (ABI, Waltham, MA) using TransStart® Green qPCR SuperMix (TransGen; catalogue number AQ101). *BnaACTIN7* was utilized as the internal control to normalize expression data according to the $\Delta\Delta C_T$ Method (Livak and Schmittgen, 2013).

Western blot

For Western blot, the total soluble protein was extracted from 300 to 500 mg 24 DAF seeds using buffer A containing 50 mM Tris-HCl 7.5, 10 mM KCl, 1 mM EDTA, 0.5 mM phenylmethanesulfonyl fluoride (PMSF), 2 mM dithiothreitol (DTT) and protease inhibitors (Thermo Scientific, Waltham, MA, catalogue number PF200523). 50 µg protein was separated by 10% SDS-PAGE gel and the protein was transferred to the PVDF membrane. The membrane was immunoblotted with an anti-Flag antibody (Sigma, St. Louis, MO, catalogue number A3687). At last, the target BASS2 protein of 45 KD was detected and positive OE lines were obtained.

Identification of Cas9-edited mutants

To obtain mutants of *BnaBASS2*, primers were used to detect Cas9 in T0 transformed individual plants first, then the PCR product including sgRNA target sequence was amplified and sent to a sequence. Eventually, Cas9 edited mutations were analysed and acquired by DSDecode (Liu et al., 2015b). After multiple generations of breeding and identification, homozygous mutants of *BnaBASS2* were obtained. Notably, the identification of mutants showed that only one target site on the eighth exon was edited and another target had no editing.

Procedure of developing seed collection

In full bloom, select a well-grown plant and pinch off the 2–3 flowers that have recently opened, and then gently tie a wire between the open flower and the flower bud (Figure S12a). Four to five individual plant replicates were selected for WT, OE, and mutant lines, and each plant was labelled with the main branch and three branches. The individual plants were bagged and selfed, and the selfing bag was removed after 4 days (Figure S12b). The seeds close to the wire are the rapeseed seeds we want to take for the specified development days.

Chloroplast isolation from developing seeds

Intact chloroplasts of 31 DAF seeds were isolated according to the previous study with modifications (Zhang, 2010; Figure S4). One gram of rapeseed seeds were placed in 4 mL of well-prechilled organelle isolation buffer (300 mM sorbitol, 50 mM Tris-HCl PH 8.0, 50 mM EDTA PH8.0) and ground into a homogenate. The homogenate of seeds was filtered by a 300-

mesh sieve (Figure S4a). The homogenate was centrifuged at 2000 g at 4 °C for 10 min, and the resulting precipitate was the crude chloroplast extract (Figure S4b). The crude extract was re-suspended in 300 µL of organelle isolation buffer and overlaid on a sucrose gradient (320 µL of 52% sucrose at the bottom and 280 µL of 30% sucrose at the top; Figure S4c). After centrifugation at 13,800 g at 4 °C for 1 h, the green bands at the interface between 52% sucrose and 30% sucrose were intact chloroplasts (Figure S4d). Chloroplasts were collected and chloroplasts examination was performed under an optical microscope to check the integrity (Figure S4e). Finally, isolated chloroplasts were precipitated and collected for the following experiments (Figure S4f).

Metabolite extraction and analysis

The metabolites involved in glycolysis and FA pathways were extracted and determined by LC-MS/MS according to previous research with modifications (Guo et al., 2014; Luo et al., 2007). Briefly, whole seeds and isolated chloroplasts of 31 DAF seeds were collected and freeze-dried (Millrock Technology, Kingston, NY). Five milligram of samples was weighed, and a mix of 1.8 mL methanol:chloroform (7:3, v/v) was added. Samples were incubated for 2 h at −20 °C and gently mixed several times during the incubation. 1.6 mL ddH₂O was added and samples were vortexed and centrifuged at 100 g for 5 min. The upper was transferred into a new tube and dried using nitrogen. The extracts were re-dissolved with 200 µL ddH₂O and then filtered with 0.45 µm cellulose acetate centrifuge tube filters. The re-dissolved extracts were used for metabolites analysis by LC-MS/MS (QTRAP 6500 plus). Mass signal intensity normalized by dry weight was calculated for comparing primary metabolites.

FA extraction and GC-FID analysis

5–10 mg oven-dried developing seeds or mature seeds were weighed and placed in a glass tube with Teflon-lined screw caps. 2.0 mL methanol with 5% (v/v) H₂SO₄ and 0.01% butylated hydroxyl toluene (BHT) was added. The seeds were crushed with a glass pestle, and then, 50 µL 16.2 µm heptadecanoic acid (17:0, used as an internal to quantify the FA) was added and the tube was capped tightly. Tubes were incubated at 85 °C for 2 h. Cool the samples, 2.0 mL H₂O and 2.0 mL hexane were added, vortex briefly, then centrifuged at 1000 rpm for 5 min. The upper phase (around 1 mL) was transferred to a glass vial for GC-FID analysis. The GC-FID instrument and analytical parameters were set as described previously (Tang et al., 2020).

Lipid extraction and analysis

Lipids were extracted and analysed according to the previous report (Lu et al., 2019). 5–10 mg freeze-dried seeds of 31 DAF were weighed and dropped into 4 mL isopropanol at 75 °C with 0.01% BHT for 15 min. Samples were cooled, 3 mL chloroform and 1.2 mL ddH₂O were added, and then, the samples were vortexed and agitated at room temperature for 1 h. Lipid extracts were transferred into a new glass screw-cap tube. 3 mL chloroform/methanol (2:1) with 0.01% BHT was added, and then, the tube was shaken for 30 min. The lipid extract was transferred into the glass screw-cap tube and this step is repeated several times until the seeds become white. 2 mL 1 M KCl was added to the lipid extracts and vortexed. Centrifuge at 1000 rpm for 5 min and the upper phase was discarded. 2 mL ddH₂O was added and vortexed. Centrifuge at 1000 rpm for 5 min and discard the upper phase. The whole extracts are dried with N₂ and re-

dissolved in chloroform to 5 mg/mL. The samples were prepared for analysis as follows: 210 μ L 300 mM ammonium acetate-methanol (1:20, v:v), 60 μ L 5 mg/mL extracts; then, the volume was filled with chloroform to 300 μ L. The lipids were quantified by LC-MS (TripleTOF 5600) and the level was calculated by mass signal intensity normalized by dry weight.

Plant growth conditions and traits survey

In this study, *B. napus* cultivar (cv.) Westar was used for gene cloning and genetic transformation. The seeds of WT, OE, and mutant were sown in the genetically modified field to set a plot experiment. The growth phenotypes were investigated, and the whole plants were harvested at maturity. Agronomic traits especially seed-related traits, such as silique length, seed number per silique, thousand seed weight, and the content of seed oil and protein were measured. The content of seed oil and protein was measured with a near-infrared reflectance spectroscope (Foss NIRSystems 5000; Gan *et al.*, 2003).

Measurement of photosynthetic efficiency

Seeds of WT, OE, and mutant were planted in the growth chamber PGW40 (Conviron, Surrey, BC, Canada) and its growth phenotype was observed indoors under a condition of 16 h light/8 h dark, 22/20 °C, and a relative humidity of 60%. The photosynthetic efficiency was measured using a portable photosynthesis system (LI-6800; Li-Cor, Lincoln, NE) with the parameters of 600 μ mol s⁻¹ flow rate, 60% relative humidity, 400 μ mol mol⁻¹ CO₂, 1000 rpm fan speed, 1200 μ mol m⁻² s⁻¹ light intensity, 20 °C.

Measurement of soluble sugar and starch content

Total soluble sugar and starch of seeds and leaves were measured by the anthrone method with some modification (Hong *et al.*, 2018). 80–100 mg seeds or leaves were collected and added into 25 mL ddH₂O, heating at 95 °C for 30 min. 50 μ L of supernatant was added to 400 μ L 2 mg/mL anthrone sulfuric acid, followed by heating at 95 °C for 5 min. The mix of heated supernatant and anthrone sulfuric acid was measured at the wavelength of 625 nm. The concentration of soluble sugar was calculated according to the glucose standard curve. Content of soluble sugar (mg/g) = concentration \times volume \div dry weight (DW).

The residues were dried and ground into powder. 5 mL 0.2 M KOH was added and the powder was ground into a homogenate. Then, the samples were transferred to a tube and heated at 95 °C for 30 min. 1 mL 1 M acetic acid was added and centrifuged at 12 000 rpm for 5 min. Finally, 50 μ L of supernatant was used to perform the remaining steps as the measurement for soluble sugar. The concentration of hydrolysis product glucose was calculated according to the glucose standard curve. Content of starch (mg/g) = 0.9 \times concentration \times volume \div DW.

OB observation of seeds by transmission electron microscope

Peel the rapeseed seeds carefully and the inner cotyledons were collected. Then, the cotyledons were cut into 1 \times 1 mm and fixed in 2.5% glutaraldehyde solution overnight. The preparation, sectioning, and observation of samples were completed by the electron microscope platform of Huazhong Agriculture University. A transmission electron microscope (TEM; H-7650; HITACHI,

Tokyo, Japan) was used in the research. The number and size of OBs in WT, OE5, and CR253 were counted and measured by Image J.

Primers

All primers used in the study were listed in Table S2.

Analysis of SOC and protein content

In this study, both SOC and protein data are % of dry weight, and when the data are compared, the difference was directly used as the increase (decrease).

Imaging software

In this study, the heatmap, bar chart line chart, and data difference analysis are all completed by Origin software.

Acknowledgements

This research was supported by grants from the Natural Science Foundation of China (31871658), China Postdoctoral Science Foundation (2021M691182), Postdoctoral Innovation Research Position Funding of Hubei Province, Hubei Hongshan Laboratory Research Fund (2021HSZD004), HZAU-AGIS Cooperation Fund (SZYJY2021004), and Higher Education Discipline Innovation Project (B20051).

Author contributions

L.G. conceived and supervised the study. S.T., N.G., F.P., Q.T., Y.L., and H.X. performed the experiments. S.T. analysed the data. S.T. wrote the manuscript. L.G. and S.L. revised the manuscript. All authors read and approved the manuscript.

Conflict of interest

The authors declare no conflict of interest.

References

- Adachi, S., Ohkubo, S., San, N.S. and Yamamoto, T. (2020) Genetic determination for source capacity to support breeding of high-yielding rice (*Oryza sativa*). *Mol. Breeding*, **40**, 20.
- Adhikari, N.D., Bates, P.D. and Browse, J. (2016) *WRINKLED1* rescues feedback inhibition of fatty acid synthesis in hydroxylase-expressing seeds. *Plant Physiol.* **171**, 179–191.
- Andre, C. and Benning, C. (2007) Arabidopsis seedlings deficient in a plastidic pyruvate kinase are unable to utilize seed storage compounds for germination and establishment. *Plant Physiol.* **145**, 1670–1680.
- Andre, C., Froehlich, J.E., Moll, M.R. and Benning, C. (2007) A heteromeric plastidic pyruvate kinase complex involved in seed oil biosynthesis in Arabidopsis. *Plant Cell*, **19**, 2006–2022.
- Andriotis, V.M., Pike, M.J., Bunnewell, S., Hills, M.J. and Smith, A.M. (2010) The plastidial glucose-6-phosphate/phosphate antiporter *GPT1* is essential for morphogenesis in Arabidopsis embryos. *Plant J.* **64**, 128–139.
- Baud, S., Mendoza, M.S., To, A., Harscoet, E., Lepiniec, L. and Dubreucq, B. (2007a) *WRINKLED1* specifies the regulatory action of *LEAFY COTYLEDON2* towards fatty acid metabolism during seed maturation in Arabidopsis. *Plant J.* **50**, 825–838.
- Baud, S., Wuielleme, S., Dubreucq, B., de Almeida, A., Vuagnat, C., Lepiniec, L., Miquel, M. *et al.* (2007b) Function of plastidial pyruvate kinases in seeds of *Arabidopsis thaliana*. *Plant J.* **52**, 405–419.
- Baud, S.B., Wuielleme, S., To, A., Rochat, C. and Lepiniec, L.C. (2009) Role of *WRINKLED1* in the transcriptional regulation of glycolytic and fatty acid biosynthetic genes in Arabidopsis. *Plant J.* **60**, 933–947.

- Bricker, D.K., Taylor, E.B., Schell, J.C., Orsak, T., Boutron, A., Chen, Y.C., Cox, J.E. et al. (2012) A mitochondrial pyruvate carrier required for pyruvate uptake in yeast, *Drosophila*, and humans. *Science*, **337**, 96–100.
- Cai, Y., Li, S., Jiao, G., Sheng, Z., Wu, Y., Shao, G., Xie, L. et al. (2018a) OsPK2 encodes a plastidic pyruvate kinase involved in rice endosperm starch synthesis, compound granule formation and grain filling. *Plant Biotechnol. J.* **16**, 1878–1891.
- Cai, Y., Zhang, W., Jin, J., Yang, X., You, X., Yan, H., Wang, L. et al. (2018b) OsPK α 1 encodes a plastidic pyruvate kinase that affects starch biosynthesis in the rice endosperm. *J. Integr. Plant Biol.* **60**, 1097–1118.
- Dai, C., Li, Y., Li, L., Du, Z. and Lu, S. (2020) An efficient *Agrobacterium*-mediated transformation method using hypocotyl as explants for *Brassica napus*. *Mol. Breeding*, **40**, 96.
- Eastmond, P.J. and Rawsthorne, S. (2000) Coordinate changes in carbon partitioning and plastidial metabolism during the development of oilseed rape embryos. *Plant Physiol.* **122**, 767–774.
- Furumoto, T. (2016) Pyruvate transport systems in organelles: future directions in C4 biology research. *Curr. Opin. Plant Biol.* **31**, 143–148.
- Furumoto, T., Yamaguchi, T., Ohshima-Ichie, Y., Nakamura, M., Tsuchida-Iwata, Y., Shimamura, M., Ohnishi, J. et al. (2011) A plastidial sodium-dependent pyruvate transporter. *Nature*, **476**, 472–U131.
- Gan, L., Sun, X., Jin, L., Wang, G., Xu, J., Wei, Z. and Fu, T. (2003) Establishment of math models of NIRS analysis for oil and protein contents in seed of *Brassica napus*. *Sci. Agric. Sin.* **36**, 1609–1613.
- Gao, X., Yan, P., Shen, W., Li, X., Zhou, P. and Li, Y. (2013) Modular construction of plasmids by parallel assembly of linear vector components. *Anal. Biochem.* **437**, 172–177.
- Guo, L., Ma, F., Wei, F., Fanella, B., Allen, D.K. and Wang, X. (2014) Cytosolic phosphorylating glyceraldehyde-3-phosphate dehydrogenases affect *Arabidopsis* cellular metabolism and promote seed oil accumulation. *Plant Cell*, **26**, 3023–3035.
- Herzig, S., Raemy, E., Montessuit, S., Veuthey, J.L., Zamboni, N., Westermann, B., Kunji, E.R. et al. (2012) Identification and functional expression of the mitochondrial pyruvate carrier. *Science*, **337**, 93–96.
- Hilgers, E.J.A., Schottler, M.A., Mettler-Altmann, T., Krueger, S., Dormann, P., Eicks, M., Flugge, U.I. et al. (2018a) The combined loss of triose phosphate and xylulose 5-phosphate/phosphate translocators leads to severe growth retardation and impaired photosynthesis in *Arabidopsis thaliana* *tpt/xpt* double mutants. *Front. Plant Sci.* **9**, 1331.
- Hilgers, E.J.A., Staehr, P., Flugge, U.I. and Hausler, R.E. (2018b) The xylulose 5-phosphate/phosphate translocator supports triose phosphate, but not phosphoenolpyruvate transport across the inner envelope membrane of plastids in *Arabidopsis thaliana* mutant plants. *Front. Plant Sci.* **9**, 1461.
- Hong, Y., Yuan, S., Sun, L., Wang, X. and Hong, Y. (2018) Cytidinediphosphate-diacylglycerol synthase 5 is required for phospholipid homeostasis and is negatively involved in hyperosmotic stress tolerance. *Plant J.* **94**, 1038–1050.
- Hua, W.L.J. and Wang, H. (2016) Molecular regulation and genetic improvement of seed oil content in *Brassica napus* L. *Front. Archit. Res.* **3**, 186–194.
- Jako, C., Kumar, A., Wei, Y., Zou, J., Barton, D.L., Giblin, E.M., Covello, P.S. et al. (2001) Seed-specific over-expression of an *Arabidopsis* cDNA encoding a diacylglycerol acyltransferase enhances seed oil content and seed weight. *Plant Physiol.* **126**, 861–874.
- Judge, A. and Dodd, M.S. (2020) Metabolism. *Essays Biochem.* **64**, 607–647.
- Kelly, A.A., Shaw, E., Powers, S.J., Kurup, S. and Eastmond, P.J. (2013) Suppression of the *SUGAR-DEPENDENT1* triacylglycerol lipase family during seed development enhances oil yield in oilseed rape (*Brassica napus* L.). *Plant Biotechnol. J.* **11**, 355–361.
- Kim, M.J., Yang, S.W., Mao, H.Z., Veena, S.P., Yin, J.L. and Chua, N.H. (2014) Gene silencing of *Sugar-dependent 1* (*USDP1*), encoding a patatin-domain triacylglycerol lipase, enhances seed oil accumulation in *Jatropha curcas*. *Biotechnol. Biofuels*, **7**, 36.
- Kong, Q. and Ma, W. (2018) *WRINKLED1* as a novel 14-3-3 client: function of 14-3-3 proteins in plant lipid metabolism. *Plant Signal. Behav.* **13**, e1482176.
- Kong, Q., Yuan, L. and Ma, W. (2019) *WRINKLED1*, a “Master Regulator” in transcriptional control of plant oil biosynthesis. *Plants*, **8**, 238.
- Le, X.H., Lee, C.P. and Millar, A.H. (2021) The mitochondrial pyruvate carrier (MPC) complex mediates one of three pyruvate-supplying pathways that sustain *Arabidopsis* respiratory metabolism. *Plant Cell*, **33**, 2776–2793.
- Lee, E.J., Oh, M., Hwang, J.U., Li-Beisson, Y., Nishida, I. and Lee, Y. (2017) Seed-specific overexpression of the pyruvate transporter *BASS2* increases oil content in *Arabidopsis* seeds. *Front. Plant Sci.* **8**, 194.
- Lei, Y., Lu, L., Liu, H.Y., Li, S., Xing, F. and Chen, L.L. (2014) CRISPR-P: a web tool for synthetic single-guide RNA design of CRISPR-system in plants. *Mol. Plant*, **7**, 1494–1496.
- Li, H., Culligan, K., Dixon, R.A. and Chory, J. (1995) *CUE1*: a mesophyll cell-specific positive regulator of light-controlled gene expression in *Arabidopsis*. *Plant Cell*, **7**, 1599–1610.
- Liu, J., Hua, W., Zhan, G., Wei, F., Wang, X., Liu, G. and Wang, H. (2010) Increasing seed mass and oil content in transgenic *Arabidopsis* by the overexpression of *wri1*-like gene from *Brassica napus*. *Plant Physiol. Bioch.* **48**, 9–15.
- Liu, F., Xia, Y., Wu, L., Fu, D., Hayward, A., Luo, J., Yan, X. et al. (2015a) Enhanced seed oil content by overexpressing genes related to triacylglyceride synthesis. *Gene*, **557**, 163–171.
- Liu, W., Xie, X., Ma, X., Li, J., Chen, J. and Liu, Y.G. (2015b) DSDecode: a web-based tool for decoding of sequencing chromatograms for genotyping of targeted mutations. *Mol. Plant*, **8**, 1431–1433.
- Liu, D., Yu, L., Wei, L., Yu, P., Wang, J., Zhao, H., Zhang, Y. et al. (2021) BnTIR: an online transcriptome platform for exploring RNA-seq libraries for oil crop *Brassica napus*. *Plant Biotechnol. J.* **19**, 1895–1897.
- Livak, K.J. and Schmittgen, T.D. (2013) Analysis of relative gene expression data using real-time quantitative PCR and the 2(-Delta Delta C(T)) Method. *Methods*, **25**, 402–408.
- Lu, S., Liu, H., Jin, C., Li, Q. and Guo, L. (2019) An efficient and comprehensive plant glycerolipids analysis approach based on high-performance liquid chromatography–quadrupole time-of-flight mass spectrometer. *Plant Direct*. **3**, e00183.
- Luo, B., Groenke, K., Takors, R., Wandrey, C. and Oldiges, M. (2007) Simultaneous determination of multiple intracellular metabolites in glycolysis, pentose phosphate pathway and tricarboxylic acid cycle by liquid chromatography-mass spectrometry. *J. Chromatogr. A*. **1147**, 153–164.
- Manan, S., Ahmad, M.Z., Zhang, G., Chen, B., Haq, B.U., Yang, J. and Zhao, J. (2017) Soybean *LEC2* regulates subsets of genes involved in controlling the biosynthesis and catabolism of seed storage substances and seed development. *Front. Plant Sci.* **8**, 1604.
- Mu, J., Tan, H., Zheng, Q., Fu, F., Liang, Y., Zhang, J., Yang, X. et al. (2008) *LEAFY COTYLEDON1* is a key regulator of fatty acid biosynthesis in *Arabidopsis*. *Plant Physiol.* **148**, 1042–1054.
- Niewiadomski, P., Knappe, S., Geimer, S., Fischer, K., Schulz, B., Unte, U.S., Rosso, M.G. et al. (2005) The *Arabidopsis* plastidic glucose 6-phosphate/phosphate translocator *GPT1* is essential for pollen maturation and embryo sac development. *Plant Cell*, **17**, 760–775.
- Pfeil, B.E., Schoefs, B. and Spetea, C. (2014) Function and evolution of channels and transporters in photosynthetic membranes. *Cell. Mol. Life Sci.* **71**, 979–998.
- Prabhakar, V., Lottgert, T., Geimer, S., Dormann, P., Kruger, S., Vijayakumar, V., Schreiber, L. et al. (2010) Phosphoenolpyruvate provision to plastids is essential for gametophyte and sporophyte development in *Arabidopsis thaliana*. *Plant Cell*, **22**, 2594–2617.
- Rawsthorne, S. (2002) Carbon flux and fatty acid synthesis in plants. *Prog. Lipid Res.* **41**, 182–196.
- Rolletschek, H., Nguyen, T.H., Hausler, R.E., Rutten, T., Gobel, C., Feussner, I., Radchuk, R. et al. (2007) Antisense inhibition of the plastidial glucose-6-phosphate/phosphate translocator in *Vicia* seeds shifts cellular differentiation and promotes protein storage. *Plant J.* **51**, 468–484.
- Santos Mendoza, M., Dubreucq, B., Miquel, M., Caboche, M. and Lepiniec, L. (2005) *LEAFY COTYLEDON 2* activation is sufficient to trigger the accumulation of oil and seed specific mRNAs in *Arabidopsis* leaves. *FEBS Lett.* **579**, 4666–4670.
- Sattler, S.E., Gilliland, L.U., Magallanes-Lundback, M., Pollard, M. and DellaPenna, D. (2004) Vitamin E is essential for seed longevity and for preventing lipid peroxidation during germination. *Plant Cell*, **16**, 1419–1432.

- Schwender, J., Ohlrogge, J. and Shachar-Hill, Y. (2004) Understanding flux in plant metabolic networks. *Curr. Opin. Plant Biol.* **7**, 309–317.
- Shen, B., Allen, W.B., Zheng, P., Li, C., Glassman, K., Ranch, J., Nubel, D. et al. (2010) Expression of *ZmLEC1* and *ZmWRI1* increases seed oil production in maize. *Plant Physiol.* **153**, 980–987.
- Streatfield, S.J., Weber, A., Kinsman, E.A., Hausler, R.E., Li, J., Post-Beittenmiller, D., Kaiser, W.M. et al. (1999) The phosphoenolpyruvate/phosphate translocator is required for phenolic metabolism, palisade cell development, and plastid-dependent nuclear gene expression. *Plant Cell*, **11**, 1609–1622.
- Tan, H., Yang, X., Zhang, F., Zheng, X., Qu, C., Mu, J., Fu, F. et al. (2011) Enhanced seed oil production in canola by conditional expression of *Brassica napus* *LEAFY COTYLEDON1* and *LEC1-LIKE* in developing seeds. *Plant Physiol.* **156**, 1577–1588.
- Tang, S., Liu, D.X., Lu, S., Yu, L., Li, Y., Lin, S., Li, L., et al. (2020) Development and screening of EMS mutants with altered seed oil content or fatty acid composition in *Brassica napus*. *Plant J.* **104**, 1410–1422.
- To, A., Joubes, J., Barthole, G., Lecureuil, A., Scagnelli, A., Jasinski, S., Lepiniec, L. et al. (2012) *WRINKLED* transcription factors orchestrate tissue-specific regulation of fatty acid biosynthesis in Arabidopsis. *Plant Cell*, **24**, 5007–5023.
- Tovar-Mendez, A., Miernyk, J.A. and Randall, D.D. (2003) Regulation of pyruvate dehydrogenase complex activity in plant cells. *Eur. J. Biochem.* **270**, 1043–1049.
- Vanhercke, T., El Tahchy, A., Shrestha, P., Zhou, X.R., Singh, S.P. and Petrie, J.R. (2013) Synergistic effect of *WRI1* and *DGAT1* coexpression on triacylglycerol biosynthesis in plants. *FEBS Lett.* **587**, 364–369.
- Wang, Z., Wei, K., Xiong, M., Wang, J.D., Zhang, C.Q., Fan, X.L., Huang, L.C. et al. (2021) Glucan, *Water-Dikinase 1* (*GWD1*), an ideal biotechnological target for potential improving yield and quality in rice. *Plant Biotechnol. J.* **19**, 2606–2618.
- Weber, A.P.M. and Linka, N. (2011) Connecting the plastid: transporters of the plastid envelope and their role in linking plastidial with cytosolic metabolism. *Annu. Rev. Plant Biol.* **62**, 53–77.
- Xing, H.L., Dong, L., Wang, Z.P., Zhang, H.Y., Han, C.Y., Liu, B., Wang, X.C. et al. (2014) A CRISPR/Cas9 toolkit for multiplex genome editing in plants. *BMC Plant Biol.* **14**, 327.
- Yang, B., Zhang, K., Jin, X., Yan, J., Lu, S., Shen, Q., Guo, L. et al. (2021) Acylation of non-specific phospholipase C4 determines its function in plant response to phosphate deficiency. *Plant J.* **106**, 1647–1659.
- Yang, Y., Kong, Q., Lim, A.R.Q., Lu, S., Zhao, H., Guo, L., Yuan, L. et al. (2022) Transcriptional regulation of oil biosynthesis in seed plants: current understanding, applications and perspectives. *Plant Commun.* **100328**, 100328.
- Yoo, S.D., Cho, Y.H. and Sheen, J. (2007) Arabidopsis mesophyll protoplasts: a versatile cell system for transient gene expression analysis. *Nat. Protoc.* **2**, 1565–1572.
- Zhang, N. (2010) The optimized method of sucrose density gradient centrifugation to isolate intact chloroplasts. *Exp. Technol. Manag.* **27**, 3 (In Chinese).
- Zhang, F., Gao, X., Zhang, J., Liu, B., Zhang, H., Xue, J. and Li, R. (2018) Seed-specific expression of heterologous gene *DGAT1* increase soybean seed oil content and nutritional quality. *Chinese J. Biotechnol.* **34**, 1478–1490.
- Zhao, Y., Ai, X., Wang, M., Xiao, L. and Xia, G. (2016) A putative pyruvate transporter *TaBASS2* positively regulates salinity tolerance in wheat via modulation of *ABI4* expression. *BMC Plant Biol.* **16**, 109.
- Zou, M., Shi, T., Wang, W., Ding, G., Xu, F. and Shi, L. (2022) Genetic dissection of seed yield and yield-related traits in *Brassica napus* grown with contrasting nitrogen supplies. *Mol. Breeding*, **42**, 1–20.

Supporting information

Additional supporting information may be found online in the Supporting Information section at the end of the article.

Figure S1 Multiple sequence alignment of BASS2 proteins and structure similarity in *B. napus* and Arabidopsis.

Figure S2 BnaA05.BASS2 is a chloroplast membrane protein by protoplast transformation of *Arabidopsis thaliana*.

Figure S3 Sequence analysis of CRISPR target genes *BnaA05.-BASS2* and *BnaC04.BASS2-1*.

Figure S4 Procedures of seed plastid isolation.

Figure S5 DAG species content in 31 DAF seeds.

Figure S6 Expression levels of genes involved in glycolytic pathway of seeds.

Figure S7 Fatty acid composition of mature seeds was determined by GC-FID.

Figure S8 The protein (a), soluble sugar (b), and starch (c) content in mature seeds.

Figure S9 Growth phenotype in the growth chamber.

Figure S10 Phenotypic measurement of 40-day-old plants.

Figure S11 Growth phenotype at mature stage.

Figure S12 Procedures of developing seed collection.

Table S1 Measurement of agronomic traits after plants were harvested.

Table S2 Primers used in this study.